

1

2

## Electronic Supplementary Information

3

4

### **Key intermediates from simultaneous removal of NO<sub>x</sub> and chlorobenzene over a V<sub>2</sub>O<sub>5</sub>–WO<sub>3</sub>/TiO<sub>2</sub> catalyst: a combined experimental and DFT study**

6

7

8

Chuan Gao,<sup>a</sup> Guangpeng Yang,<sup>b</sup> Xu Huang,<sup>c</sup> Qilei Yang,<sup>c</sup> Bing Li,<sup>c</sup> Dong Wang,<sup>\*ab</sup> Yue Peng,<sup>c</sup>

9

Junhua Li,<sup>c</sup> Chunmei Lu<sup>a</sup> and John Crittenden<sup>b</sup>

10

11

<sup>a</sup> School of Energy and Power Engineering, Shandong University, Jinan, Shandong, 250061, China.

12

<sup>b</sup> Brook Byers Institute for Sustainable Systems and School of Civil and Environmental Engineering,

13

Georgia Institute of Technology, 828 West Peachtree Street, Atlanta, GA, 30332, USA

14

<sup>c</sup> School of Environment, Tsinghua University, Beijing, 100084, China.

15

16

**\*Corresponding author.**

17

E-mail address: [dwang473@gatech.edu](mailto:dwang473@gatech.edu) (Dong Wang)

18 **Contents**

- 19 **1. The catalytic activity measurement**
- 20 **2. Fig. S1. N<sub>2</sub>O, CO, CO<sub>2</sub>, and HCl concentrations during measurement**
- 21 **3. Fig. S2. XRD diffractograms of catalyst and the optimized structure of catalyst.**
- 22 **4. Fig. S3. PDOS of Cl 2p and N 2p (NH<sub>3</sub>) of the fresh catalyst and CB-pretreated catalyst.**
- 23 **5. Fig. S4. PDOS of N 2p (cis-N<sub>2</sub>O<sub>2</sub><sup>2-</sup>) of the fresh catalyst and CB-pretreated catalyst.**
- 24 **6. Table S1. The adsorption energy ( $E_{ads}$ ) of CB, NH<sub>3</sub>, and NO.**

25 **1. The catalytic activity measurement**

26 The catalytic performance of V<sub>2</sub>O<sub>5</sub>-WO<sub>3</sub>/TiO<sub>2</sub> was evaluated in a fixed-bed quartz  
27 reactor. 200 mg of catalyst was used in simulated flue gas ([NO] = 500 ppm, [NH<sub>3</sub>] =  
28 500 ppm, [CB] = 50 ppm, [O<sub>2</sub>] = 10 vol %, and N<sub>2</sub> as balance gas) with a gas hourly  
29 space velocity (GHSV) of 60000 mL/(g·h). The conversion of NO<sub>x</sub> and CB, and the  
30 selectivity of N<sub>2</sub>, CO<sub>2</sub>, and HCl were evaluated by the following equations:

31 
$$\text{NO}_x \text{ conversion} = \frac{C_{\text{NO}_x}^{\text{in}} - C_{\text{NO}_x}^{\text{out}}}{C_{\text{NO}_x}^{\text{in}}} \times 100\% \quad (1)$$

32 
$$\text{CB conversion} = \frac{C_{\text{CB}}^{\text{in}} - C_{\text{CB}}^{\text{out}}}{C_{\text{CB}}^{\text{in}}} \times 100\% \quad (2)$$

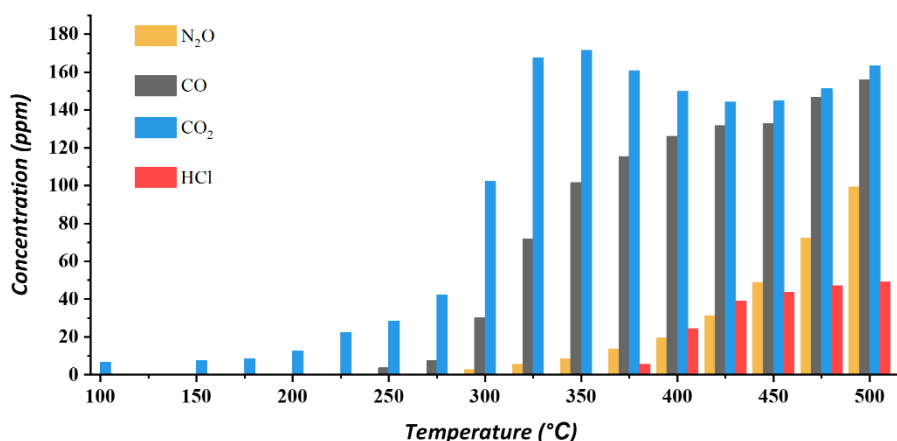
33 
$$\text{N}_2 \text{ selectivity} = \left[ 1 - \frac{2C_{\text{N}_2\text{O}}^{\text{out}}}{C_{\text{NO}_x}^{\text{in}} + C_{\text{NH}_3}^{\text{in}} - C_{\text{NO}_x}^{\text{out}} - C_{\text{NH}_3}^{\text{out}}} \right] \times 100\% \quad (3)$$

34 
$$\text{CO}_2 \text{ selectivity} = \frac{C_{\text{CO}_2}^{\text{out}}}{6 \times (C_{\text{CB}}^{\text{in}} - C_{\text{CB}}^{\text{out}})} \times 100\% \quad (4)$$

35 
$$\text{HCl selectivity} = \frac{C_{\text{HCl}}^{\text{out}}}{C_{\text{CB}}^{\text{in}} - C_{\text{CB}}^{\text{out}}} \times 100\% \quad (5)$$

36 where *in* and *out* represented the NO<sub>x</sub> concentrations of the inlet and outlet.

37



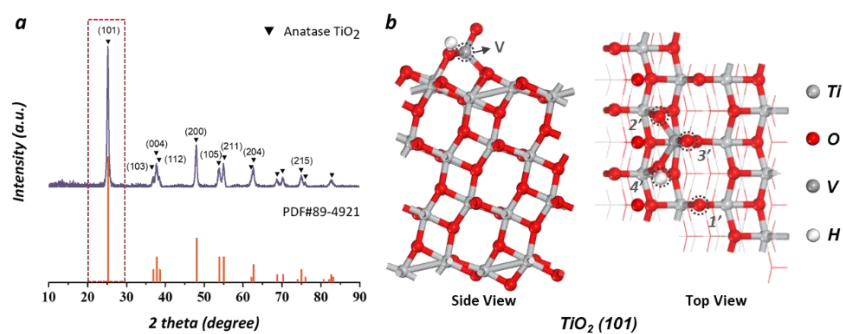
38

39 **Fig. S1.** N<sub>2</sub>O, CO, CO<sub>2</sub>, and HCl concentrations during measurement. Reaction conditions: NO 500  
 40 ppm, NH<sub>3</sub> 500 ppm, CB 50 ppm, O<sub>2</sub> 10 vol %, N<sub>2</sub> as balance gas, GHSV 60000 mL/(g·h).

41

42 The first increment at 200 – 250 °C could be assigned to the total effect of sectional  
 43 CB oxidation and CO<sub>2</sub> physical desorption. The CO<sub>2</sub> physical desorption was also  
 44 observed below 200 °C because CB conversion was zero but we could detect a trace of  
 45 CO<sub>2</sub>. A sharp drop of CO<sub>2</sub> selectivity between 250 and 275 °C could be attributed to the  
 46 completion of CO<sub>2</sub> desorption (**Fig. 1**). CO was formed in competition with CO<sub>2</sub>,  
 47 causing the decline of CO<sub>2</sub> selectivity. The second increment at 400 – 500 °C could be  
 48 due to the occurrence of Water-Gas Shift reaction converting CO to CO<sub>2</sub> which kept the  
 49 concentration of CO<sub>2</sub> and CO in balance.

50



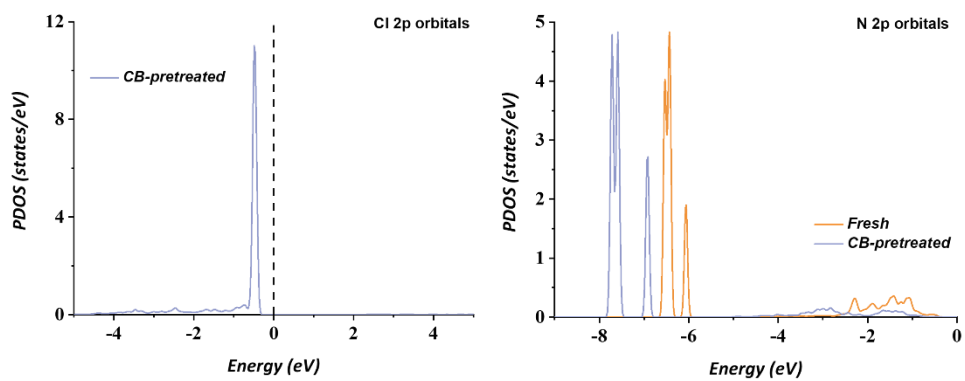
51

52 **Fig. S2.** XRD diffractograms of catalyst (a) and the optimized structure of catalyst (b).

53

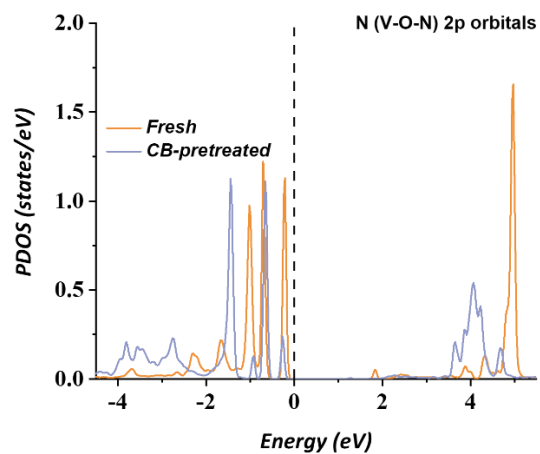
54 The characteristic peaks at 25.3°, 37.0°, 37.8°, 38.6°, 48.1°, 53.9°, 55.1°, 62.8°,  
 55 and 75.2° demonstrated that the catalyst structure was anatase TiO<sub>2</sub> phase (PDF#89-  
 56 4921). No distinct characteristic peaks of vanadium oxides were detected, implying that  
 57 these oxides were highly dispersed on TiO<sub>2</sub> support. The characteristic peak at 25.3°  
 58 was attributed to (101) plane of anatase TiO<sub>2</sub> phase. Herein, a slab model of anatase  
 59 TiO<sub>2</sub>(101) surface was selected in this calculation. The V atom was fixed on the surface  
 60 by three coordinated O atoms and H atom was bonded to O atom of V-O-Ti to form  
 61 bridge hydroxyl structure according to previous work. The optimized structure was  
 62 shown in **Figure S2 b** and four sites were considered in which *1'*, *2'*, *3'*, and *4'*  
 63 represented Ti-O-Ti, V-O-Ti, V=O, and V-O(H)-Ti, respectively.

64



65 **Fig. S3.** PDOS of Cl 2p and N 2p (NH<sub>3</sub>) of the fresh catalyst and CB-pretreated catalyst.

66

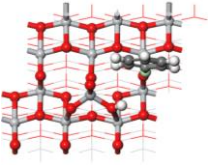
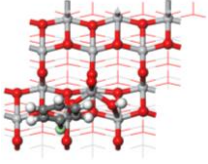
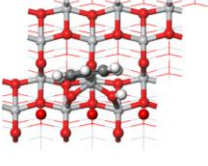
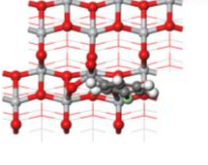
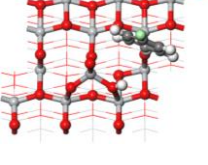
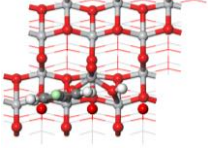
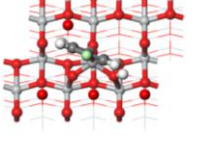
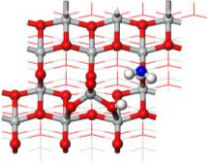
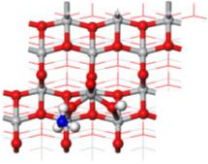
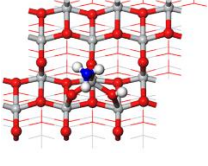
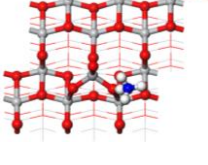
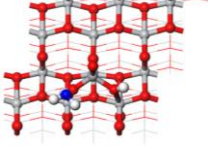
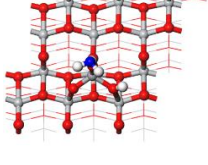
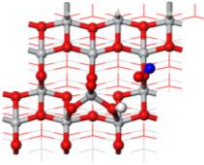
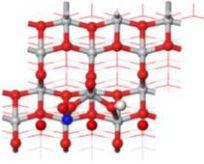
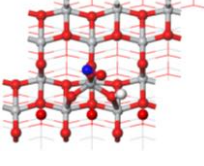
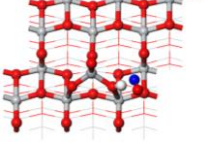
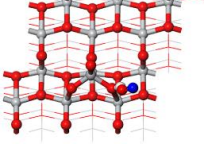


67

68 **Fig. S4.** PDOS of N 2p (*cis*-N<sub>2</sub>O<sub>2</sub><sup>2-</sup>) of the fresh catalyst and CB-pretreated catalyst.

69

70 **Table S1.** The adsorption energy ( $E_{ads}$ ) of CB, NH<sub>3</sub>, and NO.

Site <sup>a</sup>	Cl-1'	Cl-2'	Cl-3'	Cl-4'	H-1'	H-2'	H-3'
$E_{ads}$ of CB (eV)	-0.1027	0.0018	-0.0047	-0.0876	-0.0576	-0.0158	-0.043
Optimized Structure							
Site	N-1'	N-2'	N-3'	N-4'	H-2'	H-3'	
$E_{ads}$ of NH <sub>3</sub> (eV)	-0.0913	-0.0217	0.0159	-0.7059	-0.0217	-0.0319	
Optimized Structure							
Site	N-1'	N-2'	N-3'	N-4'	O-4'		
$E_{ads}$ of NO (eV)	-0.4193	-0.4515	-0.4391	-0.5121	-0.4231		
Optimized Structure							

<sup>a</sup> represented the way of molecules adsorption on surface. For example, Cl-1' represented CB adsorbing on 3' site by Cl atom and its  $E_{ads}$  is -0.1027 eV.